Thermochimica Acta, 139 (1989) 121–132
Elsevier Science Publishers B.V., Amsterdam – Printed in The Netherlands

THERMODYNAMIC STUDY ON CAMPHOR CRYSTALS *

T. NAGUMO **, T. MATSUO and H. SUGA

Department of Chemistry and Chemical Thermodynamics Laboratory, Faculty of Science, Osaka University, Toyonaka, Osaka 560 (Japan)

(Received 31 May 1988)

ABSTRACT

Heat capacities of D and D,L-camphors were measured using an adiabatic calorimeter in the temperature range between 13 and 375 K. The transition temperature between the low-temperature phase III and the room-temperature phase II of the racemic crystal was found to increase by more than 10 K when annealed at just below the apparent transition temperature. Phase III without annealing was anomalous in its calorimetric behaviour in the temperature range 70–100 K and had an excess entropy of 1.6 ± 0.4 J K^{-1} mol^{-1} at 0 K over that of the well-annealed sample. These observations were explained in terms of positional (chiral) and orientational disorder of the constituent enantiomers in the crystalline lattice. The racemic camphor, when cooled in a normal way, was found to provide us with a new example of glassy crystals.

INTRODUCTION

Molecular crystals offer a large variety of disordered systems [1]. Camphor crystallizes into a face-centred cubic system below the melting temperature. Optical enantiomers, D- and L-camphors, form a complete solid solution. On cooling the cubic phase (I), it transforms into a hexagonal phase (II) with the transition temperatures continuously changing over the whole concentration range. The low symmetry of chiral molecules and the low entropy changes associated with the fusion and transition, clearly indicate that the camphor crystals in phase II belong to the category of orientationally disordered crystals [2].

The formation of complete solid solutions of optical enantiomers is an uncommon phenomenon and is believed to be associated with dynamic disorder of the constituent molecules in the lattice [3]. Actually, D-camphor

---

* Contribution No. 150 from the Chemical Thermodynamics Laboratory. Dedicated to Professor E.F. Westrum, Jr., on the occasion of his seventieth birthday in honour of his many scientific contributions.

** Present address: Central Research Laboratory, Hitachi Ltd., Kokubunji, Tokyo.

transforms at 244.6 K into a tetragonal phase (III) on further cooling via a first-order phase transition, while D,L-camphor exhibits a higher-order phase transition at 204 K. Schäfer and his collaborators have assumed the real existence of residual entropy in D,L-camphor [4], but concluded, in a second study [5], that D- and D,L-camphors had their ordered lattices at 0 K.

There are pronounced differences in the transitional behaviour between D- and D,L-camphors. X-ray study [6] shows that the diffraction pattern changes for D-camphor on passing through the II–III transitions whereas, there is little change for D,L-camphor. The NMR second moment of D-camphor changes discontinuously at the II–III transition, while that of D,L-camphor changes gradually over a wide range of temperature [6]. The dielectric constant of D-camphor becomes small in phase III, while that of D,L-camphor remains high and exhibits noticeable dielectric dispersion at low temperatures [7,8]. These observations suggest some disorder still remaining in the low-temperature phase III of D,L-camphor [1] and are not in accord with the calorimetric conclusion [5]. This contradiction motivated us to reinvestigate the thermodynamic study of camphor crystals, particularly the thermal behaviour of the racemic camphor around the III–II transition.

EXPERIMENT

Both D- and D,L-camphors were purchased from Wako Pure Chem. Co. Ltd. They were recrystallized from hexane and then from ethanol solutions. The products were sublimed in vacuo at 50 ° C. They were finally purified by 25 passages of zone-melting in a Pyrex tube. The central part of the tube was cut off and the sample was again sublimed in vacuo.

Prior to the heat capacity measurement, the thermal behaviour of the camphor crystals was surveyed using a homemade DTA apparatus [9], which is simply designed for low temperature observations and is composed of a copper block and sample tubes [10]. The copper block is hung in a glass mantle connected to a vacuum line. To investigate the aging effect on the sample, the temperature of the copper block was regulated to ±0.2 K at each stage of the annealing process.

Heat capacities of D- and D,L-camphors were measured in the temperature range between 13 and 375 K using an adiabatic calorimeter with a built-in cryo-refrigerator [11]. The calorimeter operated effectively in long-annealing experiments at temperatures as low as 70 K. The amount of sample was 20.2365 g (0.13293 mol) for D,L-camphor and 19.7712 g (0.12987 mol) for D-camphor. The sample was sealed in a calorimetric cell together with 10^5 Pa helium gas as the heat exchanger.

The heat capacity was measured using a discontinuous heating mode comprising repeated cycles of two successive periods of heating and equilibration [12]. The temperature-drift rate of the calorimeter cell including the sample, owing to natural heat leakage, is of the order of several mK h^{-1}. Any temperature drift beyond this value arises from enthalpy relaxation occurring in the sample. The anomalous temperature drifts observed in the temperature range 70–100 K and around the III–II transition of D,L-camphor will be described later.

EXPERIMENTAL RESULTS

D-camphor showed normal transition behaviour essentially the same as that reported in the literature [5]. However, D,L-camphor behaved anomalously around the III–II transition, as revealed by the DTA experiment. DTA curves of D,L-camphor with various thermal treatments are reproduced in Fig. 1. All the curves were plotted with increasing temperature after the sample had been cooled to about 180 K with an average rate of −1 K min^{-1}. Curves A and B were taken immediately after the cooling. It was

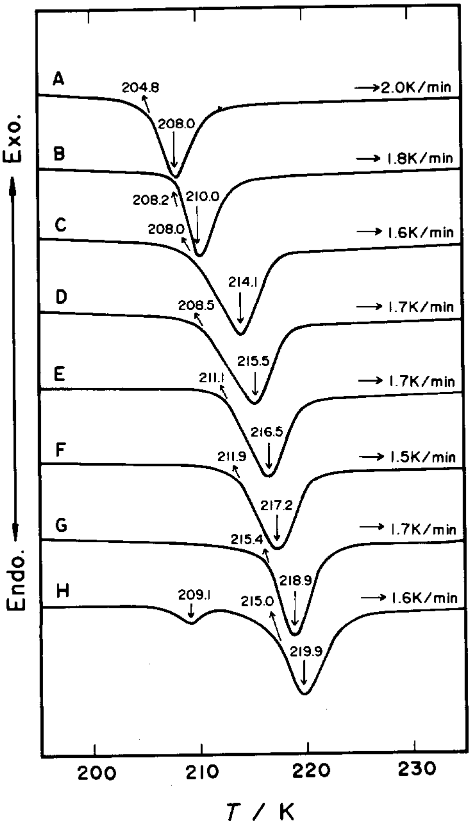

Fig. 1. DTA curves of D,L-camphor.

noticed that the transition temperature varied with different heating rates: the slower the heating rate, the higher the transition temperature. The shift of transition temperature with increasing heating rate was in the opposite direction to that which sometimes took place in the solid–solid phase transition and which may be a superheating phenomenon.

Curves C, D, and E were taken after annealing at 204.8 K for 10 h, 20 h, and 33 h, respectively. Curve F was for a specimen annealed at 209 K for 1.6 h followed by annealing at 210 K for 5.8 h. A more complex annealing was done for curve G specimen; 204.8 K for 17.8 h + 208.2 K for 12.3 h + 209.8 K for 10.3 h. Curve H was taken after annealing at 212.7 K for 13 h. It was apparent that the transition temperature shifted upward when the annealing temperature was higher and the annealing time was increased. It was believed that part of the specimen in experiment H transformed into phase II before the aging effect started so that the curve exhibited two peaks. The lower peak corresponded to that part without aging and the higher one with aging effect.

The transition temperature shifted by about 10 K as a result of this short annealing. This was really an unexpected result. Something happened during the annealing process. This observation explains why the literature value of the III–II transition temperature of the racemic camphor scatters widely between 203 K [13] and 210 K [4], in contrast to that of D-camphor.

Based on these observations, two series of heat capacity measurements were made for the racemic camphor. Series 1 was for the sample cooled with a rate of -1 K min^{-1}. The sample corresponded to that without annealing and is referred to hereafter as III$_r$ in the sense that the sample was cooled rapidly. As the temperature reached around 190 K, spontaneous temperature rise was observed in each equilibration period. The exothermic process became intense when the sample approached the III–II transition temperature of 204 K, determined previously by calorimetry [5]. The determination of equilibrium heat capacity of this sample in the III–II transition was practically impossible. It was apparent that some stabilization processes took place in the sample and caused the shift in the transition temperature.

Series 2 was for the well-annealed sample (hereafter III$_a$). The annealing was done using a series of short-interval heating cycles, ΔT, followed by annealing for Δt at that temperature. The process was started at 200 K with $\Delta T = 2$ K and $\Delta t = 2 \sim 32$ h. This cycle was continued up to 205 K when the temperature step ΔT was decreased to $0.2 \sim 0.5$ K. The procedure was again continued up to 212.4 K, when the exothermic process practically ceased. The sample III$_a$ thus annealed was cooled slowly to 13 K and the heat capacity measurement was started. The total annealing required almost one month.

Selected values of the experimental heat capacities of D- and D,L-camphors are listed in Tables 1 and 2, and they are reproduced in Fig. 2 as a function of temperature. For the calculation of heat capacity, the raw data

TABLE 1

Selected data of molar heat capacities of D-camphor

T_{av} (K)	C_p ($\mathrm{J\,K^{-1}\,mol^{-1}}$)	T_{av} (K)	C_p ($\mathrm{J\,K^{-1}\,mol^{-1}}$)	T_{av} (K)	C_p ($\mathrm{J\,K^{-1}\,mol^{-1}}$)
14.50	8.639	133.04	110.8	244.21	26399
15.77	10.28	137.06	113.6	244.36	10641
16.84	11.74	141.07	116.5	246.67	378.2
18.30	13.74	145.04	119.3	248.14	228.7
20.25	16.44	149.02	122.2	251.12	229.4
22.42	19.26	152.99	125.0	253.11	229.5
24.34	21.69	156.97	127.7	256.10	230.6
27.12	24.95	160.94	130.5	259.09	231.6
29.40	27.55	164.92	133.3	262.08	232.6
31.34	29.62	168.90	136.1	266.26	233.9
34.22	32.58	172.88	138.9	270.26	235.4
36.15	34.45	176.94	142.7	274.24	236.7
38.11	36.29	180.99	145.6	278.23	238.0
40.80	38.69	182.98	144.6	282.21	239.7
43.68	41.18	184.97	144.5	286.19	241.4
46.56	43.66	188.95	148.6	290.18	242.9
49.36	46.05	192.60	152.9	296.15	245.4
52.02	48.32	196.73	156.0	300.13	247.3
53.38	49.49	200.71	158.8	304.11	248.8
58.85	53.95	204.69	161.8	310.08	251.7
61.59	56.14	208.67	164.7	316.05	254.6
64.34	58.29	212.65	167.8	320.03	256.2
67.12	60.54	216.63	170.7	324.01	258.3
69.96	62.83	220.61	173.9	329.98	261.4
72.91	65.20	222.01	174.8	333.96	263.3
75.87	67.58	225.46	177.6	339.93	266.4
79.09	70.13	228.48	179.9	341.92	267.5
83.03	73.25	230.48	181.6	345.90	269.5
87.09	76.43	232.47	183.0	349.89	272.0
89.05	77.97	234.96	185.2	353.80	273.3
93.00	81.04	237.45	187.3	359.77	276.7
96.94	84.09	239.44	189.3	362.32	277.8
100.89	87.14	241.05	191.0	365.07	279.4
104.85	90.14	243.12	195.5	368.56	281.3
108.80	93.11	243.57	976.6	370.41	282.2
112.76	96.08	243.87	3888	371.39	463.0
116.72	99.04	243.91	4084	371.66	593.9
118.70	100.5	243.94	6069	371.89	439.5
120.68	101.9	244.02	7537	372.61	280.1
127.01	106.5	244.07	10446	373.38	279.2
129.07	107.9	244.12	26693	374.15	281.3
				374.85	280.1

were corrected for the effect of vaporization inside the sample cell [13]. D-camphor behaved normally in a sense that any annealing effect was not observed. The maximum heat capacity was obtained at 244.19 K, which was taken as the transition temperature of the enantiomeric crystal.

It is important to mention here the low temperature behaviour of the phase III_r. A sample annealed, for example at 72 K for 65 h, exhibited

TABLE 2

Selected data of molar heat capacities of D,L-camphor

T_{av} (K)	C_p ($J\ K^{-1}\ mol^{-1}$)	T_{av} (K)	C_p ($J\ K^{-1}\ mol^{-1}$)	T_{av} (K)	C_p ($J\ K^{-1}\ mol^{-1}$)
Series 1 (rapidly-cooled specimen)		94.88	88.56	185.53	186.7
		96.67	90.56	187.97	189.0
14.94	11.15	97.56	91.37	190.01	193.1
16.05	12.71	99.36	93.27	193.01	199.4
18.80	16.70	101.15	95.16	196.02	207.2
20.51	19.14	103.83	98.04	198.05	213.0
23.18	22.68	105.62	99.96	201.12	223.5
25.79	25.92	107.41	101.9	204.25	233.3
29.32	30.00	110.09	104.7	205.03	232.9
31.33	31.89	112.78	107.5	218.09	251.3
33.77	34.63	115.47	110.2	220.37	250.7
36.41	37.19	118.16	112.8	222.68	249.4
38.18	38.83	120.85	115.4	225.07	247.1
40.83	41.18	122.02	116.5	227.45	245.3
42.60	42.61	124.43	118.9	229.24	244.3
45.26	44.97	127.97	122.2	231.03	243.3
47.04	46.51	129.95	124.1	234.71	241.4
49.84	48.87	133.92	127.8	237.90	240.5
52.51	51.14	137.89	131.5	240.28	239.9
55.23	53.40	141.85	135.3	243.46	238.8
57.01	54.87	145.82	139.1	246.81	238.8
59.67	57.11	147.80	141.1	249.49	238.6
62.34	59.47	149.85	143.1	252.17	238.2
64.13	61.04	151.85	145.0	255.55	238.7
66.76	63.35	153.90	147.1	260.02	239.4
69.42	65.56	155.87	149.0	264.06	239.5
71.24	67.11	158.31	151.6	268.47	240.5
72.99	68.62	161.70	155.2	272.70	241.1
74.42	69.88	165.52	159.3	276.68	242.2
76.01	71.27	169.64	164.1	281.79	244.0
78.40	73.30	171.59	166.4	285.48	244.8
80.78	75.38	172.58	167.6	288.72	246.1
83.20	77.55	175.57	171.5	293.02	247.8
85.58	79.72	177.56	174.3	279.30	249.5
87.97	81.96	179.55	177.0	301.55	251.2
90.36	84.23	181.54	180.1	305.79	252.8
93.07	86.88	183.53	183.3	310.00	255.1

TABLE 2 (continued)

T_{av} (K)	C_p (J K^{-1} mol^{-1})	T_{av} (K)	C_p (J K^{-1} mol^{-1})	T_{av} (K)	C_p (J K^{-1} mol^{-1})
316.27	257.9	83.23	76.84	187.55	175.1
322.48	260.5	85.53	78.86	190.55	178.3
362.24	281.1	87.21	80.36	193.54	181.7
366.14	283.8	90.40	83.25	196.18	184.9
367.10	289.1	93.54	86.17	199.33	188.8
367.72	648.5	96.72	89.09	201.73	192.3
368.05	395.3	99.08	91.19	204.12	195.9
368.85	283.8	101.46	93.53	207.24	201.0
370.40	282.9	104.65	96.42	210.02	206.3
373.30	284.5	107.05	98.52	212.10	210.8
		109.44	100.6	215.44	218.8
Series 2 (well-annealed specimen)		112.63	103.4	218.42	228.6
		115.02	105.5	221.19	240.0
35.82	36.26	118.22	108.3	224.19	263.3
37.48	37.81	121.43	111.1	225.11	271.0
39.25	39.43	124.62	114.0	225.62	278.2
41.27	41.25	127.01	116.1	225.96	369.4
43.01	42.76	130.20	119.0	226.33	458.3
45.18	44.56	133.69	122.1	226.35	405.8
47.27	46.23	136.65	124.8	226.46	306.1
49.74	48.33	140.64	128.5	226.93	282.8
52.15	50.39	143.63	131.3	227.50	259.3
55.73	53.44	146.62	134.1	228.48	254.9
57.53	55.01	149.61	137.0	229.54	250.2
59.92	57.01	152.60	139.8	230.22	248.1
62.32	59.07	154.59	141.8	230.57	246.2
64.70	61.08	157.67	144.8	231.34	245.3
66.50	62.61	160.65	147.7	232.11	244.2
68.29	64.06	163.64	150.8	233.65	243.1
70.09	65.69	166.63	153.7	234.43	242.4
72.84	68.00	169.62	156.8	235.36	241.8
74.28	69.22	172.62	159.8	238.24	240.7
75.25	70.04	175.61	162.9	241.20	240.1
77.27	71.73	178.60	165.8	244.28	239.1
79.08	73.26	181.59	169.0	247.25	238.8
81.51	75.36	184.54	171.9	251.22	238.7

strong endothermic effects in the subsequent several equilibration periods. When the temperature drift returned to normal at around 80 K, a second annealing was done. Again, strong endothermic effects were observed in the equilibration periods. The effect was observed between 70 and 100 K. A partially frozen enthalpy relaxed towards an equilibrium value during the annealing, and the untraceable enthalpy during the following heatings relaxed towards a new equilibrium value by showing the endothermic effect under the adiabatic condition. If the dielectric data [7] are extrapolated to

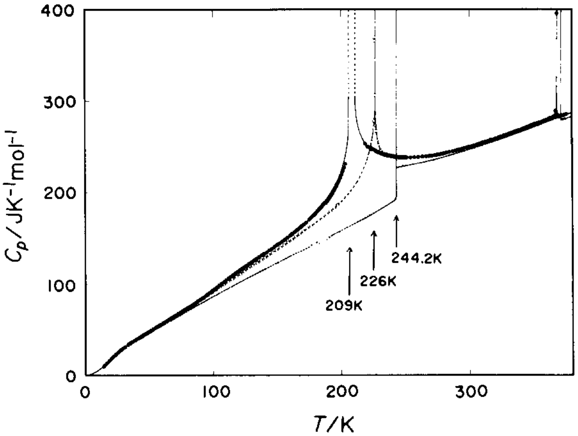

Fig. 2. Molar heat capacities of D- and D,L-camphor crystals, quenched and annealed.

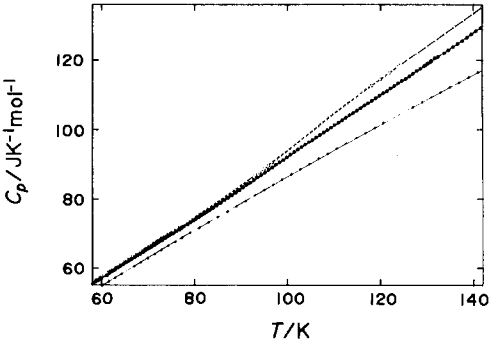

Fig. 3. Molar heat capacities of D- and D,L-camphor crystals, quenched and annealed: ◆———◆, D-camphor; ●———●, D,L-camphor quenched; ○———○, D,L-camphor annealed.

low temperatures, the dielectric relaxation time becomes 10^4 s at 90 K, a value corresponding to the time scale of a single heat capacity measurement. On the other hand, phase $\mathrm{III_a}$ does not show any enthalpy relaxation in the relevant temperature ranges. At the same time, the heat capacities of phase $\mathrm{III_a}$ were smaller than those of phase $\mathrm{III_r}$, as shown in Fig. 3. Obviously the low-temperature enthalpy relaxation disappeared as a result of the annealing done at around the III–II transition.

DISCUSSION

There seems to be two kinds of ordering process in the racemic crystal of camphor occurring around the III–II transition region, each possessing

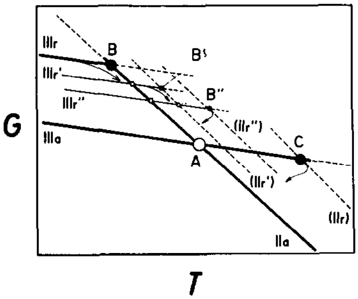

Fig. 4. Schematic Gibbs energy curves of D,L-camphor crystals.

completely different time scales. In order to understand these unusual findings, it is necessary to recall the fact that the racemic modification is an equimolecular mixture of the two enantiomers, D- and L-camphors. Both of the optical isomers are believed to be located on the hexagonal lattice points in a completely random way in phase II by virtue of the orientational disorder. It is believed that orientational ordering takes place first on cooling the D,L-camphor crystal, leaving the chiral disorder behind. This kind of chirality problem cannot happen in the lattice of D-camphor. Because D- and L-camphor molecules have different spatial conformations, molecular packing in the temporarily ordered state will not be suitable to attain the lowest energy. Some molecules will have misorientation owing to the positional disorder. Spatial rearrangement of both the enantiomers requires a diffusional process of each molecule, and therefore the chiral ordering takes place slowly.

A schematic diagram of Gibbs energy of D,L-camphor is illustrated in Fig. 4. Point A is the hypothetical thermodynamic transition temperature between the disordered and ordered phases with respect to both of the relevant degrees of freedom. The phase II_a will transform into III_r at point B on cooling. The phase is orientationally ordered and positionally disordered for a moment. Then the phase III_r stabilizes to III'_r by a short aging. The new phase III'_r transforms at point B′ into phase II'_r, which has the corresponding order with orientational disorder, and then relaxes towards the phase II_a. The well-annealed phase III_a will transform into phase II_r at point C and then relax towards the phase II_a for the same reason. The diffusional process will be enhanced in the phase II because of the translation–rotation coupling. Because of the single peak observed in the DTA curves for each stage of aging, the positional ordering is considered to take place uniformly in the phase III_r. Thus an innumerable number of Gibbs energy curves corresponding to each stage of positional ordering is believed to exist between the phases III_r and III_a. This conjecture was actually confirmed by the observation of strong endothermic temperature drifts during the III_a–II transition region. The effect culminated when the calorimetric specimen reached 226 K, when the apparent heat capacity attained a maximum value.

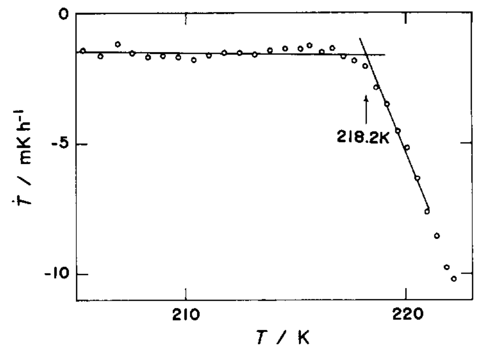

Fig. 5. Spontaneous temperature-drift rate of well-annealed D,L-camphor around the III–II transition region.

This superheating effect makes it difficult to determine experimentally the equilibrium transition temperature. We have to rely on other experiments for that determination. Figure 5 gives the temperature-drift rates observed in each equilibration period of the heat capacity measurement of the well-annealed D,L-camphor. The rates changed discontinuously at 218.2 K and this was regarded as an indication of the onset of instability of the phase III_a during warming. More evidence of this was given by the following observations. The sample of D,L-camphor in phase II_a was cooled rapidly to 224 K when its heat capacity measurement drew attention to the temperature-drift behaviour. The operation was repeated by changing the lowest temperature step-by-step by 2 K. When the lowest temperature was 218 K, the drift behaviour changed suddenly. This temperature was accepted as an indicator of loss of stability of the phase II_a. We accepted 218.2 K as the thermodynamic temperature of the transition between the phases III_a and II_a.

The determination of the equilibrium transition temperature enables us to calculate the entropy change along the thermodynamic path. Referring to the entropy at 298.15 K, the entropy changes along the III_r–II and III_a–II thermodynamic paths are: $\Delta_0^{298.15}$ S(D,L-camphor, III_r–II) = (290.15 ± 0.2) J K^{-1} mol^{-1}; $\Delta_0^{298.15}$ S(D,L-camphor, III_a–II) = (291.76 ± 0.2) J K^{-1} mol^{-1}; and $\Delta_0^{298.15}$ S(D-camphor, III–II) = (289.76 ± 0.2) J K^{-1} mol^{-1}.

The change of estimated equilibrium transition temperature by ±1 K induces change in the ΔS value by ±0.03 J K^{-1} mol^{-1}. The hypothetical transition temperature between the phase II_a and III_r (point B in Fig. 4) is difficult to determine experimentally. This is because the enthalpy relaxation takes place during the initial cooling and the subsequent heating. In the absence of any other clear evidence, we simply assigned the transition temperature as 209.12 K, at which the main part of the III_r–II transition started to occur. In view of an irreversible entropy production [14] during the cooling and heating experiments, we can conclude that at least 1.6 J K^{-1} mol^{-1} of entropy was removed from D,L-camphor by the aging. The disorder

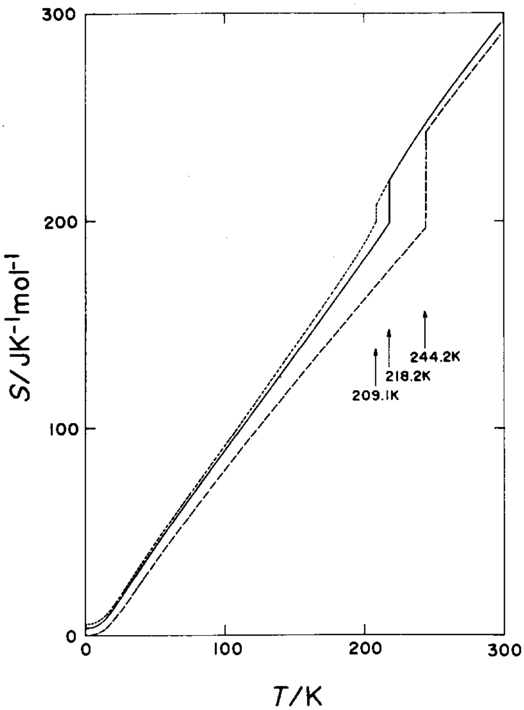

Fig. 6. Molar entropies of D- and D,L-camphor crystals quenched and annealed: — — —, D-camphor; ———, D,L-camphor annealed; - - - - - -, D,L-camphor quenched.

corresponding to this entropy may be the main origin of the different low temperature behaviours between D- and D,L-camphors that have been reported hitherto.

Schäfer and his collaborators have concluded that the camphor crystal is an ideal solid–solution system [4]. This conclusion is based on the observations that the vapour pressures and enthalpies of sublimation of D- and D,L-camphors are essentially the same at room temperature within their experimental errors. If this conclusion is correct, we can compare the absolute entropies of the enantiometric and racemic crystals of camphor. The D,L-camphor crystal should have excess entropy of R ln 2, corresponding to the ideal mixing, over that of D-camphor at 298.15 K. Based on the assumption that the enantiometric crystal obeys the third law of thermodynamics, the entropy curves of both crystals are drawn in Fig. 6. The calculation does not necessarily mean that the well-annealed D,L-camphor crystal has a residual entropy. This is because the estimated error of enthalpy of sublimation by ± 2 kJ mol^{-1} corresponds to ± 6.7 J K^{-1} mol^{-1} in the determination of entropy difference. We must rely on other techniques for the comparison of absolute entropies of both camphor crystals. It is possible that the removal of chiral disorder is not complete in the "well-annealed" specimen of racemic crystal. Again we can conclude that the unannealed D,L-camphor crystal does not obey the third law of thermodynamics.

In this way, the racemic crystal of camphor cooled in a normal way has a residual entropy of at least 1.6 ± 0.4 J K^{-1} mol^{-1}, and shows an enthalpy relaxation around 70–100 K. The dielectric relaxation can be correlated with the enthalpy relaxation and will be associated with the freezing-out of remaining orientational disorder coupled with the positional disorder. In this sense, the normally-cooled D,L-camphor belongs to a new category of glassy crystals [15] which are chirally disordered and orientationally partially-ordered. All the low temperature studies of D,L-camphors have been done on samples without aging, that is, with the sample in a glassy crystalline state. A theoretical consideration of the phase diagram of D- and D,L-camphors [16] is based on observation of a sample which is not in thermodynamic equilibrium. We are now beginning to experiment on chiral substances with orientationally disordered phases.

It is interesting to infer the ordered structure of the phase II_a of racemic camphor. A superstructure is suggested [17] because there is no indication of phase separation of both enantiomeric crystals. Structural analysis of the well-aged D,L-camphor using X-ray or neutron diffraction methods merits further study.

REFERENCES

1 N.G. Parsonage and L.A.K. Staveley, Disorder in Crystals, Clarendon Press, Oxford, 1978.
2 J. Timmermans, J. Phys. Chem. Solids, 18 (1961) 1.
3 B. Chion, J. Lajzerowicz, D. Bordeaux, A. Collet and J. Jacques, J. Phys. Chem., 82 (1978) 2682.
4 K.L. Schäfer and P. Frey, Z. Elektrochem., 56 (1952) 882.
5 K.L. Schäfer and U. Wagner, Z. Elektrochem., 62 (1958) 328.
6 J.E. Anderson and W.P. Slichter, J. Chem. Phys., 41 (1964) 1922.
7 W.A. Yager and S.O. Morgan, J. Am. Chem. Soc., 57 (1935) 2071.
8 V. Rossiter, J. Phys. C, 5 (1972) 1969.
9 H. Suga, H. Chihara and S. Seki, Nippon Kagaku Zasshi (J. Chem. Soc. Jpn.), 82 (1960) 24.
10 H. Suga and S. Seki, Thermochim. Acta, 100 (1986) 149.
11 K. Moriya, T. Matsuo and H. Suga, J. Chem. Thermodyn., 14 (1982) 1143.
12 H. Suga and S. Seki, Faraday Discuss. Chem. Soc., 69 (1980) 221.
13 J.P. McCullough, in D.W. Scott (Ed.), Experimental Thermodynamics, Vol. 1, Calorimetry of Non-reacting Systems, Butterworths, London, 1968.
14 R.O. Davies and G.O. Jones, Proc. R. Soc. London, Ser. A, 217 (1953) 26.
15 H. Suga and S. Seki, J. Non-Cryst. Solids, 16 (1974) 171.
16 C.C. Mjojo, J. Chem. Soc., Faraday Trans. II, 75 (1978) 667.
17 B. Chion and J. Lajzerowicz-Bonneteau, in J. Lascombe (Ed.), Dynamics of Molecular Crystals, Elsevier, 1987, 285 pp.